Increase in the acousto-optic figure of merit in SiO_2 crystals due to optical activity. Anisotropic acousto-optic interactions

Mys O., Adamenko D. and Vlokh R.

O. G. Vlokh Institute of Physical Optics, 23 Dragomanov Street, 79005 Lviv, Ukraine

Received: 04.08.2023

Abstract. We analyze anisotropic acousto-optic (AO) interactions of three possible acoustic eigenwaves with the incident and diffracted optical eigenwaves elliptically polarized due to optical activity effect in quartz crystals. Dependences of the effective elasto-optic (EO) coefficient and the AO figure of merit on the diffraction angle are obtained. We demonstrate that proper accounting for a nonzero ellipticity of the optical eigenwaves leads to nonzero values of some effective EO coefficients and a presence of the corresponding AO interactions of so-called types VII and VIII. We also reveal the effect of non-orthogonality of the acoustic waves on the effective EO coefficient and the AO figure of merit at the AO interactions of the types VII and VIII. The ellipticity of the optical eigenwaves manifests itself in peak-like angular maxima of the effective EO coefficient and the AO figure of merit for all the types of AO interactions under consideration. These maxima appear around the diffraction angles 0 and 180 deg that correspond to the collinear AO interaction between the circularly polarized optical waves propagating along the optic axis. The maximal values of the AO figure of merit in this case are respectively equal to 1.16×10^{-15}, 0.36×10^{-15} and 0.48×10^{-15} s^3/kg at the types VII, VIII and IX of AO interactions. Finally, we show that a deviation of the incidence angle from 90 deg at the interaction types VII and VIII leads to zeroing of the effective EO coefficient and the AO figure of merit.

Keywords: acousto-optic diffraction, anisotropic diffraction, diffraction efficiency, quartz crystals, optical activity, ellipticity of optical eigenwaves

UDC: 535.43, 535.551, 535.562, 534-16

1. Introduction

In our recent works [1, 2], we have shown that proper consideration of a nonzero ellipticity of optical eigenwaves caused by an optical activity effect can enhance the efficiency of acousto-optic (AO) Bragg diffraction. The reason is that additional components of elasto-optic (EO) tensor are involved in the effective EO coefficient p_{eff} due to the optical activity in crystals. The AO figure of merit depends on p_{eff} according to the relation [3]

$$M_2 = \frac{n_i^3 n_d^3 p_{eff}^2}{\rho v^3}, \tag{1}$$

where n_i and n_d are the refractive indices associated respectively with the incident and diffracted optical waves, v denotes the velocity of an acoustic wave (AW) and ρ is the crystal density.

In fact, this phenomenon has been observed for the first time in Ref. [4] in paratellurite crystals. Then the AO figure of merit increases from $(600–800)\times10^{-15}$ s^3/kg for the linearly polarized interacting optical waves up to 1200×10^{-15} s^3/kg for the circularly polarized optical

eigenwaves. This occurs when the incident optical beam propagates in a relatively small angular vicinity of an optic axis. Another example where this phenomenon has been observed is optically biaxial and optically active α-HIO_3 crystals. Here the AO efficiency also increases significantly whenever the incident and diffracted optical waves propagate along the directions close to the optic axis [5]. In our recent work [1], we have determined experimentally the effective EO coefficients for the case of AO interactions of linearly and circularly polarized optical waves in optically active $Pb_5Ge_3O_{11}$ crystals. Moreover, a clear increase in the effective EO coefficients has been found for these crystals.

We have shown earlier that the enhancement of the AO efficiency is peculiar for all the types of AO interactions, including isotropic and anisotropic ones. However, the work mentioned above has operated with approximate relations obtained for the effective EO coefficient for the case of anisotropic diffraction. Namely, the cross section of the characteristic surface for the extraordinary refractive index n_e has been regarded as a circle. In addition, the diffraction angle has been assumed to be very small and constant. In Ref. [6], we have analyzed the influence of ellipticity of optical eigenwaves on the AO figure of merit in quartz crystals only for the case of isotropic AO Bragg diffraction. In spite of this shortage, a noticeable fact has been found: the AO figure of merit increases by 54% for the AO interactions of the n_o-polarized optical wave with the quasi-longitudinal (QL) AW. In the case of AO interactions of the n_e-polarized optical wave with the QL AW, the above parameter demonstrates more than threefold increase. A similar situation occurs for the AO interactions with the quasi-transverse (QT) AW denoted as QT_1, of which polarization belongs to the *YZ* plane. In particular, the peak value of the AO figure of merit for the AO interactions with the n_o-polarized optical wave increases by 19%, while the corresponding AO figure of merit increases by more than the order of magnitude.

Since α-SiO_2 crystals represent a very important optical material used in different optical and piezoelectric devices [7–12], in the present work we consider the anisotropic AO Bragg diffraction in these crystals and its enhancement due to a nonzero ellipticity of optical eigenwaves caused by the natural optical activity. Below we will consider the anisotropic AO diffraction with taking into account of the changes in the diffraction angle and with accounting for the phase-matching conditions following from the actual shape of wave-vector surfaces in optically active crystals.

2. Method of analysis

α-SiO_2 crystals belong to the point symmetry group 32. They can exist in two enantiomorphous modifications that differ by their signs of optical rotation. The crystals are optically active, with the specific rotation equal to $\rho = 18.8$ deg/ mm at the optical wavelength $\lambda = 632.8$ nm [13]. The gyration-tensor components at this wavelength are equal to $g_{33} = (10.06 \pm 0.07) \times 10^{-5}$ and $g_{11} = (-4.8 \pm 0.5) \times 10^{-5}$ for a dextrorotary modification of the crystals [14] which is considered in the present work. The refractive indices for the linearly polarized optical waves amount to $n_o = 1.543$ and $n_e = 1.552$ [15]. The components of the EO tensor p_{ij} at $\lambda = 538$ nm are as follows: $p_{11} = 0.16$, $p_{13} = 0.27$, $p_{12} = 0.27$, $p_{14} = -0.030$, $p_{31} = 0.29$, $p_{33} = 0.10$, $p_{41} = -0.047$ and $p_{44} = -0.079$ (it is supposed that the dispersion of the EO coefficients is weak enough in the region 538–632.8 nm). The elastic stiffnesses C_{lj} are given by $C_{11} = 87.486$, $C_{33} = 107.2$, $C_{12} = 6.244$, $C_{13} = 11.91$, $C_{44} = 57.98$, $C_{66} = 40.626$ and $C_{14} = -18.09$ GPa [16, 17]. All of these coefficients have been measured under the condition of constant electric induction. Finally, the density of α-SiO_2 amounts to $\rho = 2649$ kg/m^3.

The *Z* and *X* axes of the optical indicatrix for α-SiO_2 are parallel respectively to the three-fold and two-fold symmetry axes, while the *Y* axis is perpendicular to the *XZ* plane. In our analysis, we will consider anisotropic AO interactions between the optical waves and the QL, QT and purely transverse (PT) AWs propagating in the *YZ* plane. Let us notice that the eigenvectors of the Christoffel tensor in the *YZ* plane are rotated only about the *X* axis so that the solutions for the eigenvalues of this tensor can be obtained analytically. It is not so for the *XZ* plane.

The ellipticity of the incident (the index '*i*') and diffracted (the index '*d*') optical eigenwaves are given by the relations [18]

$$\chi_i = \frac{1}{2G(\varphi_i)}\left((n_o^2 - \mathrm{n}'^2_e) - \sqrt{(n_o^2 - \mathrm{n}'^2_e) + 4G(\varphi_i)^2}\right) \approx \frac{G(\varphi_i)}{n_o^2 - n'^2_e}, \tag{2}$$

$$\chi_d = \frac{1}{2G(\varphi_d)}\left((n_o^2 - \mathrm{n}'^2_e) - \sqrt{(n_o^2 - \mathrm{n}'^2_e) + 4G(\varphi_d)^2}\right) \approx \frac{G(\varphi_d)}{n_o^2 - n'^2_e}, \tag{3}$$

where *G* is the scalar gyration parameter and φ_i and φ_d are the angles between the *Y* axis and the propagation directions of the incident and diffracted optical waves, respectively (see Fig. 1). Note that the parameters involved in Eqs. (2) and (3) are given by

$$G(\varphi_i) = g_{33}\sin^2(\varphi_i) + g_{11}\cos^2(\varphi_i) \tag{4}$$

for the incident optical wave and

$$G(\varphi_d) = g_{33}\sin^2\varphi_d + g_{11}\cos^2\varphi_d \tag{5}$$

for the diffracted optical wave, with $\varphi_d = \varphi_i + \gamma$ and γ being the angle of diffraction. The corresponding refractive indices read as

$$\mathrm{n}'^2_e(\varphi_i) = \frac{n_o^2 n_e^2}{n_o^2\cos^2\varphi_i + n_e^2\sin^2\varphi_i} \tag{6}$$

for the incident optical wave and

$$\mathrm{n}'^2_e(\varphi_d) = \frac{n_o^2 n_e^2}{n_o^2\cos^2\varphi_d + n_e^2\sin^2\varphi_d} \tag{7}$$

for the diffracted wave.

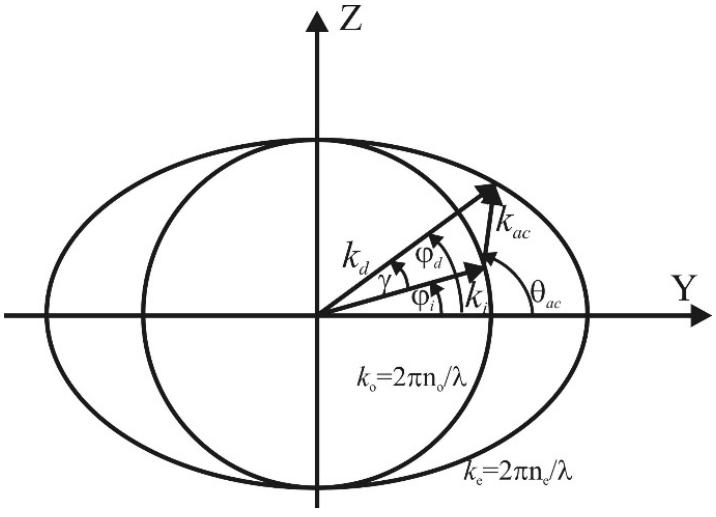

Fig. 1. Schematic vector diagram of anisotropic AO interactions in SiO_2 crystals.

Let the diffracted optical wave propagate at the angle γ with respect to the wave vector of the incident wave (see Fig. 1). Here the incident wave is assumed to be polarized as the ordinary wave (i.e., parallel to the *X* axis). Then the diffracted wave is polarized as the extraordinary one, so that its polarization vector belongs to the *YZ* plane and remains perpendicular to the wave vector of the diffracted wave. Since the ellipticity of the optical eigenwaves is small enough at $96 \text{ deg} \le \varphi_i \le 84 \text{ deg}$ (and the same holds true at $276 \text{ deg} \le \varphi_i \le 264 \text{ deg}$) [18], we will consider only the angular region $90 \text{ deg} \le \varphi_i \le 84 \text{ deg}$. For each φ_i value, which we change in the region $90 \text{ deg} \le \varphi_i \le 84 \text{ deg}$ with the step 1 or 2 deg, the angle γ changes by 360 deg (with the step 1 deg) in such a way that the wave vector of the diffracted wave rotates anticlockwise.

As seen from Fig. 1, the direction of the AW vector changes when the angle φ_i does. For instance, we deal with the collinear AO diffraction whenever γ is equal to 0 or 180 deg. Then the three wave vectors (i.e., the wave vectors of the two optical waves and the AW) remain collinear. This kind of AO interactions cannot be accomplished at $\varphi_i = 90$ or 270 deg as long as we disregard a circular optical birefringence, since the linear birefringence is equal to zero along these directions. The direction of the AW vector is determined uniquely by the angle θ_{ac} between the AW vector and the *Y* axis:

$$\theta_{ac} = \pi + \arctan\left\{\frac{\left(\dfrac{(n_o + A)(n_o + B)}{\sqrt{\cos^2\varphi_d\,(n_o + B)^2 + \sin^2\varphi_d\,(n_o + A)^2}}\right)\sin\varphi_d - \left(\dfrac{(n_o - A)(n_o - B)}{\sqrt{\cos^2\varphi_i\,(n_o - B)^2 + \sin^2\varphi_i\,(n_o - A)^2}}\right)\sin\varphi_i}{\left(\dfrac{(n_o + A)(n_o + B)}{\sqrt{\cos^2\varphi_d\,(n_o + B)^2 + \sin^2\varphi_d\,(n_o + A)^2}}\right)\cos\varphi_d - \left(\dfrac{(n_o - A)(n_o - B)}{\sqrt{\cos^2\varphi_i\,(n_o - B)^2 + \sin^2\varphi_i\,(n_o - A)^2}}\right)\cos\varphi_i}\right\}, \tag{8}$$

where the *A* and *B* parameters are given by the relations $A = \dfrac{g_{11}^2}{2n_o(n_e^2 - n_o^2)}$ and $B = \dfrac{g_{33}^2}{2n_o(n_e^2 - n_o^2)}$.

Note that the addition of π at $\gamma = 0$ should be omitted since we have $\varphi_d = \varphi_i + \gamma$.

The relations for the AW velocities for different principal planes in the crystals have been presented in the recent work [6]. Then the polarization of the AW QT_1 responsible for the type VIII of AO interactions lies in the *YZ* plane. In contrast, the polarization of the AW PT_2 participating in the AO interactions of the type IX remains PT and perpendicular to the *YZ* plane. Then the strain-tensor components caused by the QL AWs and the AWs QT_1 at the types VII and VIII of AO interactions are respectively given by [1]

$$e_2 = e_0 \cos\theta_{ac} \cos\xi,\ e_3 = e_0 \sin\theta_{ac} \sin\xi,\ e_4 = e_0 \sin(\theta_{ac} + \xi), \tag{9}$$

$$e_2 = -e_0 \cos\theta_{ac} \sin\xi,\ e_3 = e_0 \sin\theta_{ac} \cos\xi,\ e_4 = e_0 \cos(\theta_{ac} + \xi), \tag{10}$$

where

$$\xi = 0.5\,\mathrm{atan}\left[\frac{2C_{24}\cos^2\theta_{ac} + (C_{13}+C_{44})\sin 2\theta_{ac}}{(C_{11}-C_{44})\cos^2\theta_{ac} + (C_{44}-C_{33})\sin^2\theta_{ac} + 0.5C_{24}\sin 2\theta_{ac}}\right] \tag{11}$$

denotes the angle between the displacement vector and the Y axis, whereas e_0 is the unit strain. The effective EO coefficient can be written as

$$p_{eff} = \sqrt{(E_2^2 + E_3^2)\chi_d^2 + E_2^2 + E_3^2}\,, \tag{12}$$

where

$$\begin{aligned} E_1 &= \Delta B_{11}\sin\delta_1 + \Delta B_{12}\chi_i \sin\delta_2 \sin\varphi_i + \Delta B_{13}\chi_i \sin\delta_2 \cos\varphi_i, \\ E_2 &= \Delta B_{12}\sin\delta_1 + \Delta B_{22}\chi_i \sin\delta_2 \sin\varphi_i + \Delta B_{23}\chi_i \sin\delta_2 \cos\varphi_i, \\ E_3 &= \Delta B_{13}\sin\delta_1 + \Delta B_{23}\chi_i \sin\delta_2 \sin\varphi_i + \Delta B_{33}\chi_i \sin\delta_2 \cos\varphi_i \end{aligned} \tag{13}$$

are the components of the electric-field strength of the diffracted optical wave for the types VII and VIII of AO interactions. Here δ_1 is the phase of the X-polarized incident wave and δ_2 denotes the phase of the Y- and Z-polarized incident waves. Finally, the increments of components of the dielectric impermeability tensor read as

$$\begin{aligned} &\Delta B_{11} = p_{12}e_2 + p_{13}e_3 + p_{14}e_4, \quad \Delta B_{12} = 0, \\ &\Delta B_{22} = p_{22}e_2 + p_{23}e_3 + p_{24}e_4, \quad \Delta B_{13} = 0, \quad \Delta B_{33} = p_{32}e_2 + p_{33}e_3. \end{aligned} \tag{14}$$

The strain-tensor components for the type IX of AO interactions with the AW PT_2 can be written as

$$e_6 = e_0\cos\theta_{ac}, \;\; e_5 = e_0\sin\theta_{ac}\,. \tag{15}$$

Then the increments of the impermeability-tensor components are as follows:

$$\begin{aligned} &\Delta B_{11} = p_{14}e_4, \Delta B_{22} = p_{24}e_4, \Delta B_{33} = 0, \\ &\Delta B_{12} = p_{66}e_6, \Delta B_{13} = p_{56}e_6, \Delta B_{23} = p_{44}e_4. \end{aligned} \tag{16}$$

As a result, the effective EO coefficient for the type VII of AO interactions is given by

$$\begin{aligned} p_{eff}^{2\,(VII)} = {} & 0.5\chi_i^2 \left\{ \begin{aligned} &\left(p_{44}\sin 2\theta_{ac} - p_{41}\cos^2\theta_{ac}\right)^2 \\ &+\left(p_{22}\cos^2\theta_{ac} + p_{23}\sin^2\theta_{ac} - p_{14}\sin 2\theta_{ac}\right)^2 \sin^2\varphi_i \\ &+\left(p_{31}\cos^2\theta_{ac} + p_{33}\sin^2\theta_{ac}\right)^2 + \\ &+\left(p_{22}\cos^2\theta_{ac} + p_{23}\sin^2\theta_{ac} - p_{14}\sin 2\theta_{ac}\right) \\ &\times\left((p_{31}-p_{41})\cos^2\theta_{ac} + p_{33}\sin^2\theta_{ac} + p_{44}\sin 2\theta_{ac}\right)\sin 2\varphi_i \end{aligned} \right\} \\ & +0.5\chi_i^2\chi_d^2 \left\{ \begin{aligned} &\left(p_{44}\sin 2\theta_{ac} - p_{41}\cos^2\theta_{ac}\right)^2 \\ &+\left(p_{22}\cos^2\theta_{ac} + p_{23}\sin^2\theta_{ac} - p_{14}\sin 2\theta_{ac}\right)^2 \sin^2\varphi_i \\ &+\left(p_{31}\cos^2\theta_{ac} + p_{33}\sin^2\theta_{ac}\right)^2 + \\ &+\left(p_{22}\cos^2\theta_{ac} + p_{23}\sin^2\theta_{ac} - p_{14}\sin 2\theta_{ac}\right) \\ &\times\left((p_{31}-p_{41})\cos^2\theta_{ac} + p_{33}\sin^2\theta_{ac} + p_{44}\sin 2\theta_{ac}\right)\sin 2\varphi_i \end{aligned} \right\}, \end{aligned} \tag{17}$$

when the non-orthogonality of the AWs is not taken into account. The same relation reads as

$$p_{eff}^{2\,(VII)} = 0.5\chi_i^2 \begin{Bmatrix} \left(p_{44}\sin(\theta_{ac}+\xi) - p_{41}\cos\theta_{ac}\cos\xi\right)^2 \\ +\left(p_{22}\cos\theta_{ac}\cos\xi + p_{23}\sin\theta_{ac}\sin\xi - p_{14}\sin(\theta_{ac}+\xi)\right)^2\sin^2\varphi_i \\ +\left(p_{31}\cos\theta_{ac}\cos\xi + p_{33}\sin\theta_{ac}\sin\xi\right)^2 + \\ +\left(p_{22}\cos\theta_{ac}\cos\xi + p_{23}\sin\theta_{ac}\sin\xi - p_{14}\sin(\theta_{ac}+\xi)\right) \\ \times\left((p_{31}-p_{41})\cos\theta_{ac}\cos\xi + p_{33}\sin\theta_{ac}\sin\xi + p_{44}\sin(\theta_{ac}+\xi)\right)\sin 2\varphi_i \end{Bmatrix}$$

$$+0.5\chi_i^2\chi_d^2 \begin{Bmatrix} \left(p_{44}\sin 2\theta_{ac} - p_{41}\cos\theta_{ac}\cos\xi\right)^2 + \\ +\left(p_{22}\cos\theta_{ac}\cos\xi + p_{23}\sin\theta_{ac}\sin\xi - p_{14}\sin(\theta_{ac}+\xi)\right)^2\sin^2\varphi_i \\ +\left(p_{31}\cos\theta_{ac}\cos\xi + p_{33}\sin\theta_{ac}\sin\xi\right)^2 \\ +\left(p_{22}\cos\theta_{ac}\cos\xi + p_{23}\sin\theta_{ac}\sin\xi - p_{14}\sin(\theta_{ac}+\xi)\right) \\ \times\left((p_{31}-p_{41})\cos\theta_{ac}\cos\xi + p_{33}\sin\theta_{ac}\sin\xi + p_{44}\sin(\theta_{ac}+\xi)\right)\sin 2\varphi_i \end{Bmatrix}, \quad (18)$$

when the above non-orthogonality is accounted for.

For the type VIII of AO interactions, the effective EO coefficient reads as

$$p_{eff}^{2\,(VIII)} = 0.5\chi_i^2 \begin{Bmatrix} \left(p_{44}\cos 2\theta_{ac} - p_{41}\sin 2\theta_{ac}\right)^2 \\ +\left((p_{22}-p_{23})\sin 2\theta_{ac} - p_{14}\cos 2\theta_{ac}\right)^2\sin^2\varphi_i + \left(p_{31}-p_{33}\right)^2\sin^2 2\theta_{ac} \\ +\left((p_{22}-p_{23})\sin 2\theta_{ac} - p_{14}\cos 2\theta_{ac}\right) \\ \times\left((p_{31}-p_{41}-p_{33})\sin 2\theta_{ac} + p_{44}\cos 2\theta_{ac}\right)\sin 2\varphi_i \end{Bmatrix}$$

$$+0.5\chi_i^2\chi_d^2 \begin{Bmatrix} \left(p_{44}\cos 2\theta_{ac} - p_{41}\sin 2\theta_{ac}\right)^2 \\ +\left((p_{22}-p_{23})\sin 2\theta_{ac} - p_{14}\cos 2\theta_{ac}\right)^2\sin^2\varphi_i + \left(p_{31}-p_{33}\right)^2\sin^2 2\theta_{ac} \\ +\left((p_{22}-p_{23})\sin 2\theta_{ac} - p_{14}\cos 2\theta_{ac}\right) \\ \times\left((p_{31}-p_{41}-p_{33})\sin 2\theta_{ac} + p_{44}\cos 2\theta_{ac}\right)\sin 2\varphi_i \end{Bmatrix} \quad (19)$$

with no account for the non-orthogonality and

$$p_{eff}^{2\,(VIII)} = 0.5\chi_i^2 \begin{Bmatrix} \left(p_{44}\cos(\theta_{ac}+\xi) + p_{41}\cos\theta_{ac}\sin\xi\right)^2 \\ +\left(p_{23}\sin\theta_{ac}\cos\xi - p_{22}\cos\theta_{ac}\sin\xi - p_{14}\cos(\theta_{ac}+\xi)\right)^2\sin^2\varphi_i \\ +\left(p_{33}\sin\theta_{ac}\cos\xi - p_{31}\cos\theta_{ac}\sin\xi\right)^2 + \\ +\left(p_{23}\sin\theta_{ac}\cos\xi - p_{22}\cos\theta_{ac}\sin\xi - p_{14}\cos(\theta_{ac}+\xi)\right) \\ \times\left(p_{33}\sin\theta_{ac}\cos\xi - (p_{31}-p_{41})\cos\theta_{ac}\sin\xi + p_{44}\cos(\theta_{ac}+\xi)\right)\sin 2\varphi_i \end{Bmatrix}$$

$$+0.5\chi_i^2\chi_d^2 \begin{Bmatrix} \left(p_{44}\cos(\theta_{ac}+\xi) + p_{41}\cos\theta_{ac}\sin\xi\right)^2 \\ +\left(p_{23}\sin\theta_{ac}\cos\xi - p_{22}\cos\theta_{ac}\sin\xi - p_{14}\cos(\theta_{ac}+\xi)\right)^2\sin^2\varphi_i \\ +\left(p_{33}\sin\theta_{ac}\cos\xi - p_{31}\cos\theta_{ac}\sin\xi\right)^2 \\ +\left(p_{23}\sin\theta_{ac}\cos\xi - p_{22}\cos\theta_{ac}\sin\xi - p_{14}\cos(\theta_{ac}+\xi)\right) \\ \times\left(p_{33}\sin\theta_{ac}\cos\xi - (p_{31}-p_{41})\cos\theta_{ac}\sin\xi + p_{44}\cos(\theta_{ac}+\xi)\right)\sin 2\varphi_i \end{Bmatrix}, \quad (20)$$

with consideration of this non-orthogonality. It is seen from the above formulae that the squared effective EO coefficients depend on the squared ellipticity of the incident optical wave and the multiplied squared ellipticities of the incident and diffracted waves. Moreover, the effective EO coefficients are equal to zero under the condition when the optical activity is absent and the ellipticity is zero, so that the anisotropic diffraction of these types cannot be implemented. Finally, we note that Eq. (18) reduces to Eq. (17) and Eq. (20) transforms into Eq. (19) whenever the AW non-orthogonality becomes zero (i.e., under the condition $\xi = \theta_{ac}$).

The effective EO coefficient for the type IX of AO interactions is as follows:

$$\begin{aligned} p_{eff}^{2(IX)} &= 0.5(p_{66}^2 + p_{41}^2)^2 \cos^2\theta_{ac} \\ &+0.5\chi_i^2\left((p_{44}^2 - p_{14}^2\sin^2\varphi_i - p_{16}p_{44}\sin 2\varphi_i)\sin^2\theta_{ac}\right) \\ &+0.5\chi_i^2\chi_d^2\left((p_{66}^2 + p_{41}^2)^2\cos^2\theta_{ac} + (p_{44}^2 - p_{14}^2\sin^2\varphi_i - p_{16}p_{44}\sin 2\varphi_i)\sin^2\theta_{ac}\right). \end{aligned} \tag{21}$$

Eq. (21) testifies that the type IX of AO interactions can exist even if the optical ellipticity is equal to zero. Here the term proportional to $\chi_i^2\chi_d^2$ is small enough and so one can neglect it except for the cases when the ellipticity is close to unity.

3. Results and discussion

The dependences of the squared effective EO coefficient and the AO figure of merit on the angle γ under the condition $\varphi_i = 90$ deg in the *YZ* plane for the type VII of AO interactions are presented in Fig. 2.

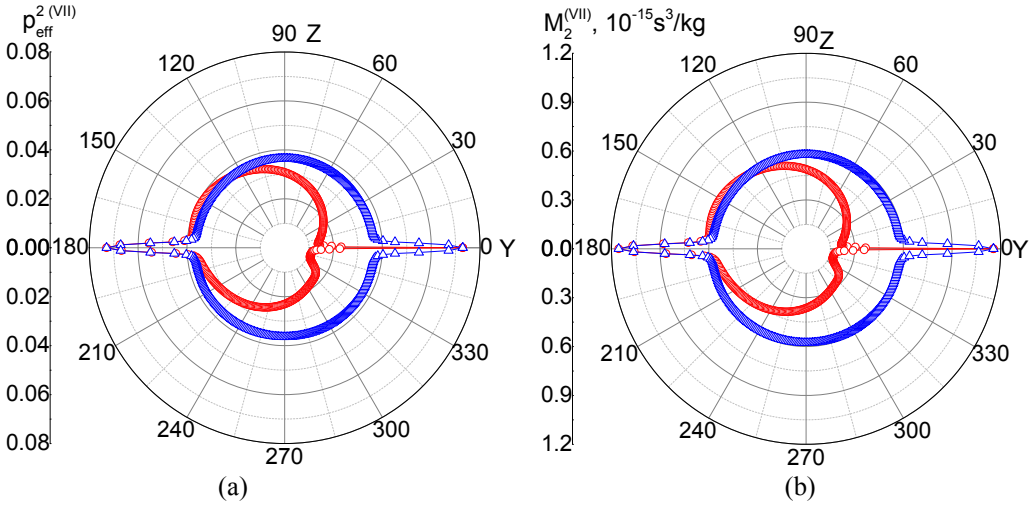

Fig. 2. Dependences of squared effective EO coefficient (a) and AO figure of merit (b) on the angle γ in the *YZ* plane for the type VII of AO interactions ($\varphi_i = 90$ deg): circles correspond to consideration of the non-orthogonality of AWs and triangles to disregard of this non-orthogonality.

As mentioned above, the type VII of AO interactions cannot be realized without accounting for the ellipticity of the optical eigenwaves, since the appropriate effective AO coefficient is equal to zero (see Eqs. (17) and (18)). One can see in Fig. 2a that accounting for the non-orthogonality of the QL AW leads to changes in the character of dependence of the effective EO coefficient on the angle γ. Moreover, consideration of the non-orthogonality of this AW results in decreased effective EO coefficient and AO figure of merit (see Fig. 2b). On the other hand, peculiar peaks of

the effective EO coefficient and the AO figure of merit arise at $\gamma = 0$ and 180 deg , i.e. under the condition when both the incident and diffracted optical waves propagate along the optic axis. These peaks are caused by the ellipticity of the optical eigenwaves, which approaches unity when the optical waves propagate along the optic axis in the optically active quartz crystals. Under this condition, the collinear AO diffraction takes place. For the collinear diffraction and the interaction between the circularly polarized optical waves, the AO figure of merit equals to 1.16×10^{-15} s^3/kg. The AO figure of merit is the highest under this condition in case of the type VII of AO interactions.

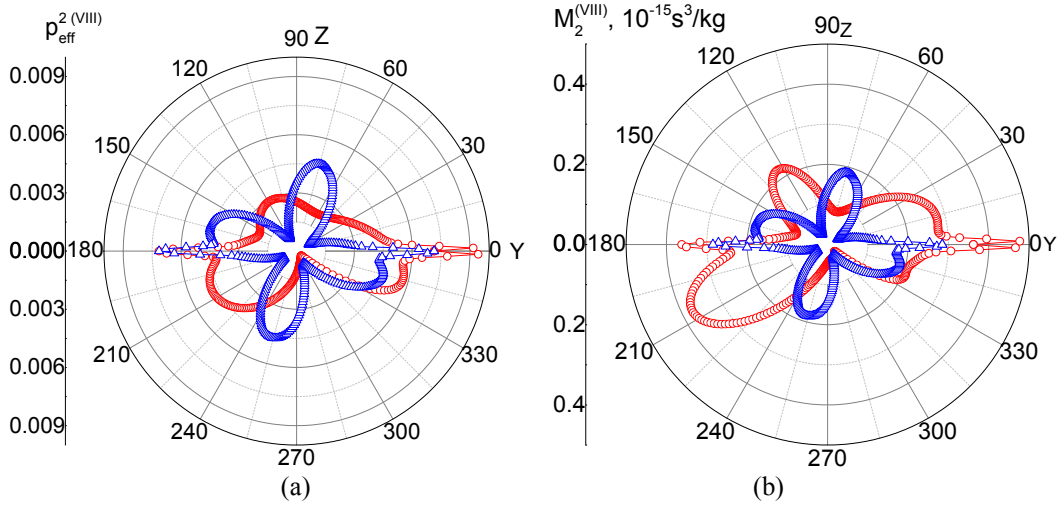

Fig. 3. Dependences of squared effective EO coefficient (a) and AO figure of merit (b) on the angle γ in the YZ plane for the type VIII of AO interactions ($\varphi_i = 90$ deg): circles correspond to consideration of the non-orthogonality of AWs and triangles to disregard of this non-orthogonality.

Accounting for the non-orthogonality of the AWs in the case of AO interactions with the AW QT_1 (see Fig. 3) leads to the result similar to that observed for the AO interactions with the QL AW. Namely, we deal with increased effective EO coefficient and AO figure of merit. Moreover, the peaks caused by the ellipticity of optical eigenwaves at $\gamma = 0$ and 180 deg are quite appreciable. These peaks appear when the optical waves propagate along the optic axis, which corresponds to the collinear AO diffraction. For this kind of diffraction, the incident (say, the right-handed) optical wave diffracts and transforms into the left-handed diffracted wave. However, in the vicinity of γ=0 deg and 180 deg, the behavior of the effective EO coefficient and AO figure of merit differ. Namely in the vicinity of γ=0 deg, the two peaks are observed while in the vicinity of γ=180 deg not. Such different behavior is caused by the different behavior of non-orthogonality angle at the approaching of γ to 0 deg and 180 deg. The AO figure of merit reaches the value of 0.36×10^{-15} s^3/kg, at the collinear type of AO interaction. However, the highest value of AO figure of merit is reached at the γ=±1 deg and is equal to 0.48×10^{-15} s^3/kg.

As mentioned above, the AW PT_2 remains PT. The AO interaction with this AW is possible even when the ellipticity of the optical eigenwaves equals zero. In the case of zero ellipticity, the effective EO coefficient and the AO figure of merit are equal to zero at $\gamma = 0$ and 180 deg (see Fig. 4). Hence, the collinear AO interaction cannot be implemented, since one cannot satisfy the phase-matching conditions when the optical waves propagate along the optic axis where both

linear and circular birefringences are equal to zero. The situation changes when the optical activity is present and the ellipticity of eigenwaves is properly considered. Then peaks are observed in the dependences of the effective EO coefficient and the AO figure of merit on the angle γ (see Fig. 4). The maximal AO figure of merit, 0.48×10^{-15} s^3/kg, is reached at the collinear diffraction.

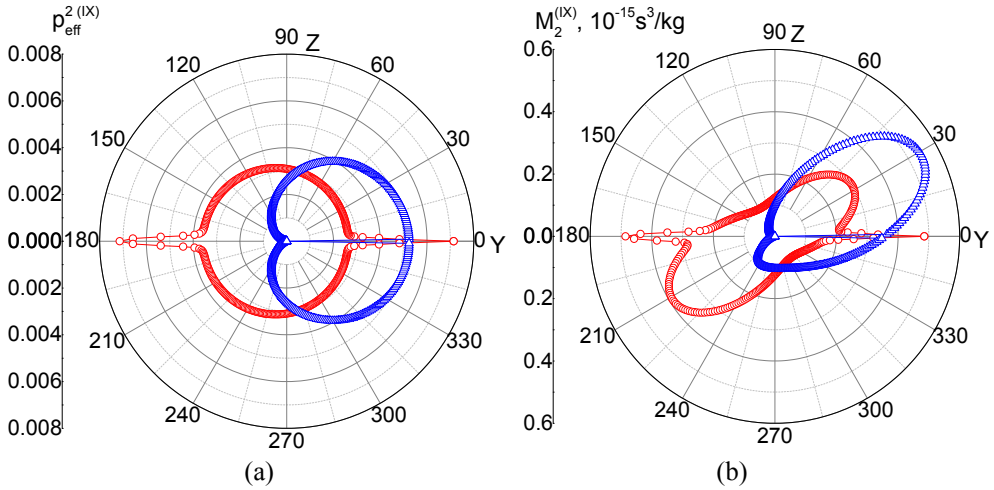

Fig. 4. Dependences of squared effective EO coefficient (a) and AO figure of merit (b) on the angle γ in the *YZ* plane for the type IX of AO interactions ($\varphi_i = 90$ deg): circles correspond to consideration of the ellipticity of optical eigenwaves and triangles to disregard of this ellipticity.

Note that the AO figures of merit obtained by us for the type VII of AO interaction in the case of collinear diffraction are relatively high. For comparison, one can remind that the AO figure of merit for the quartz crystals is extremely small, 0.06×10^{-15} s^3/kg, in the case of AO interaction of the longitudinal AW propagating along the *X* axis and the linearly polarized optical waves.

Now let us consider the influence of the changes in the incidence angle of the input optical wave on the effective EO coefficient and the AO figure of merit for the three types of anisotropic diffraction. As seen from Fig. 5 and Fig. 6, the angular peaks of the effective EO coefficient and the AO figure of merit rotate when the incidence angle of the incoming optical wave deviates from 90 deg. This rotation is given by the relation $\gamma = \varphi_d - \varphi_i$, i.e. decreasing φ_i leads to less diffraction angle γ. This situation is clearly observed in Fig. 5 and Fig. 6.

At the same time, the effective EO coefficient and the AO figure of merit approach zero with decreasing incidence angle for the types VII and VIII of AO interactions (see Fig. 7). This effect is caused by decreasing ellipticity of optical eigenwaves occurring when the incident optical wave deviates from the direction of the optic axis. As seen from Eqs. (17)–(20), the ellipticity of the incident wave contributes much more to the effective EO coefficient than the ellipticity of the diffracted wave. On the other hand, the magnitude of the peak value of the AO figure of merit at the type IX of AO interactions is almost independent of the angle $90 - \varphi_i$.

Earlier, we have studied experimentally the collinear AO diffraction in the quartz and paratellurite crystals for the case when the optical waves and the longitudinal AW propagate along the optic axis [19]. Immediately, this experiment has been carried out in order to reveal the acousto-gyration diffraction effect. However, it follows from the results of the present work that the AO diffraction with accounting for the ellipticity of optical eigenwaves should manifest itself in the same manner as the acousto-gyration diffraction. Nonetheless, no effect has been found

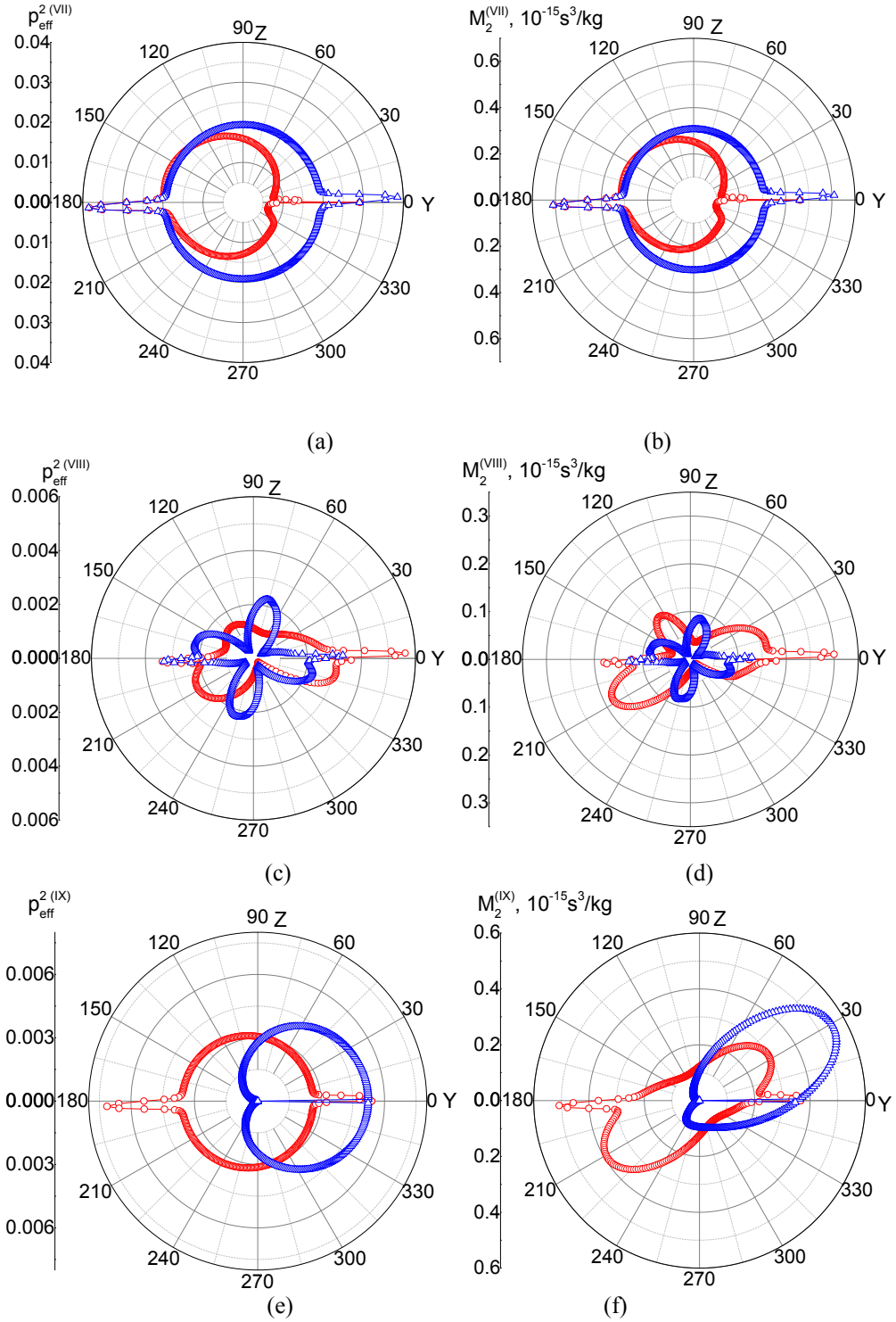

Fig. 5. Effective EO coefficients (panels a, c and e) and AO figures of merit (panels b, d and f) for the types VII (a, b), VIII (c, d) and IX (e, f) of AO interactions ($\varphi_i = 88$ deg): circles in panels (a)–(d) correspond to consideration of the non-orthogonality of AWs and triangles to disregard of this non-orthogonality; circles in panels (e) and (f) correspond to consideration of the ellipticity of optical eigenwaves and triangles to disregard of this ellipticity.

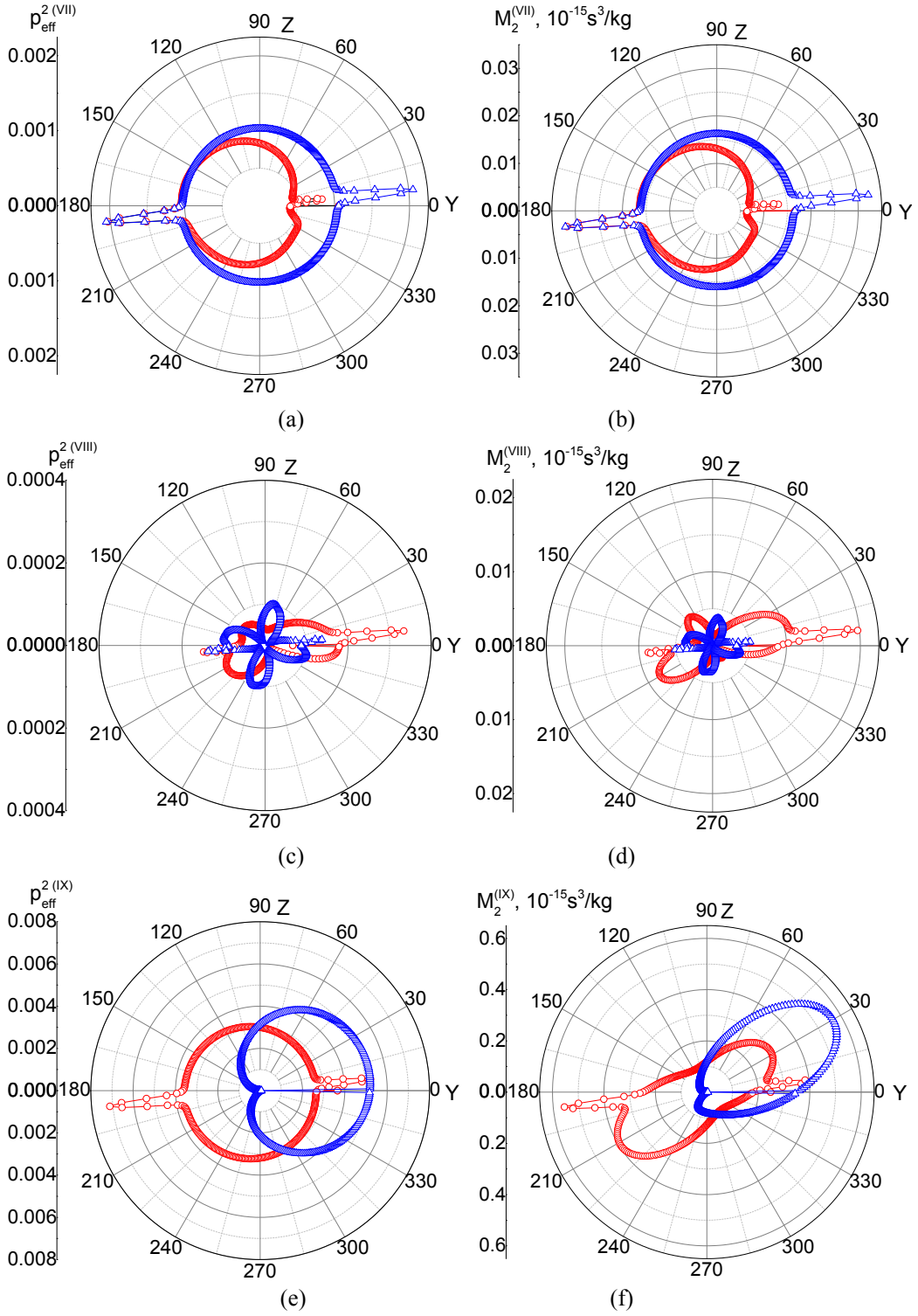

Fig. 6. Effective EO coefficients (panels a, c and e) and AO figures of merit (panels b, d and f) for the types VII (a, b), VIII (c, d) and IX (e, f) of AO interactions ($\varphi_i = 84$ deg): circles in panels (a)–(d) correspond to consideration of the non-orthogonality of AWs and triangles to disregard of this non-orthogonality; circles in panels (e) and (f) correspond to consideration of the ellipticity of optical eigenwaves and triangles to disregard of this ellipticity.

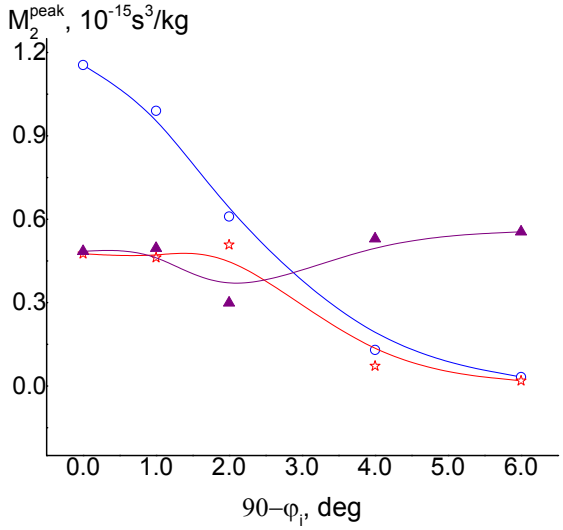

Fig. 7. Dependences of the peak magnitudes of AO figure of merit on the angle $90-\varphi_i$: circles, stars and triangles correspond respectively to the types VII, VIII and IX of AO interactions.

experimentally in Ref. [19]. A possible reason for the lack of positive results in this experiment is a relatively low acoustic power applied. As a matter of fact, the powers ~ 1–5 W are needed in order to detect the collinear AO diffraction in the quartz crystals [20].

4. Conclusions

In the present work, we have analyzed the anisotropic AO interactions with the three possible acoustic eigenwaves in the quartz crystals. This has been done with consideration of a nonzero ellipticity of the incident and diffracted optical eigenwaves, which is caused by the optical activity effect. Moreover, the analysis has been performed with accounting for the changes in the characteristic surfaces of the refractive indices (or the wave vectors) occurring due to the circular birefringence. The non-orthogonality of the AWs has also been taken into account.

We have obtained the dependences of the effective EO coefficients and the AO figures of merit on the diffraction angle. It has been found that the AO interactions cannot be implemented inside the *YZ* plane in case of the types VII and VIII of AO interactions when respectively the QL AW and the AW QT_1 are dealt with. This situation takes place as long as we disregard the ellipticity of the optical eigenwaves, since the appropriate effective EO coefficients are equal to zero in this case. However, a proper consideration of the ellipticity of optical eigenwaves gives rise to the effective EO coefficients different from zero and, as a result, to the appearance of AO interactions.

We have found that, in case of the type VII of AO interactions, accounting for the non-orthogonality of the AWs results in decreasing effective EO coefficient and AO figure of merit. Nonetheless, accounting for this effect leads to the opposite result in case of the type VIII of AO interactions. The ellipticity of the optical eigenwaves manifests itself in peak-like angular maxima of the effective EO coefficients and the AO figures of merit for all of the interaction types under consideration. These maxima appear at the diffraction angles 0 and 180 deg which correspond to the collinear AO interaction between the circularly polarized optical waves propagating along the optic axis. The maximal values of the AO figure of merit in this case are equal to 1.16×10^{-15}, 0.36×10^{-15} and 0.48×10^{-15} s^3/kg respectively at the AO interactions of the types VII, VIII and IX.

When the incidence angle of the input optical wave deviates from 90 deg, the angular orientations of the maxima corresponding to the effective EO coefficients and the AO figures of merit change by the same angle. At the same time, the magnitudes of these maxima for the types VII and VIII of AO interactions approach zero. In general, both the effective EO coefficients and the AO figures of merit collapse to zero in this case. On the other hand, the maximum of the AO figure of merit is almost independent of the deviation of the incidence angle from 90 deg whenever we deal with the type IX of AO interactions.

References

1. Mys O, Kostyrko M, Adamenko D, Martynyuk-Lototska I, Skab I and Vlokh R, 2022. Effect of ellipticity of optical eigenwaves on the enhancement of efficiency of acousto-optic Bragg diffraction. A case of optically active $Pb_5Ge_3O_{11}$ crystals. AIP Adv. **12**: 055130.
2. Mys O, Adamenko D and Vlokh R, 2023. Influence of Faraday elliptical birefringence on the acousto-optic diffraction efficiency: a case of isotropic interaction with quasi-longitudinal acoustic waves in KH_2PO_4 crystals. Ukr. J. Phys. Opt. **24**: 95–103.
3. Balakshyi V I, Parygin V N and Chirkov L E. Physical Principles of Acousto-Optics. Moscow: Radio i Svyaz, 1985.
4. Yano T and Watanabe A, 1974. Acousto-optic figure of merit of TeO_2 for circularly polarized light. J. Appl. Phys. **45**: 1243–1245.
5. Kurpeychik M I and Balakshy V I, 2018. Peculiarities of acousto-optic interaction in biaxial crystal of alpha-iodic acid. Appl. Opt. **57**: 5549–5555.
6. Mys O, Adamenko D and Vlokh R, 2023. Enhancement of acousto-optic diffraction efficiency in SiO_2 crystals due to ellipticity of optical eigenwaves: isotropic acousto-optic interaction. Ukr. J. Phys. Opt. **24**: 124–134.
7. Cady W G, 1921. The piezoelectric resonator. Phys. Rev. **17**: 531.
8. Pierce G W, 1923. Piezoelectric crystal resonators and crystal oscillators applied to the precision calibration of wavemeters. Proc. Amer. Acad. Arts Sci. **59**: 81–106.
9. Lombardi M, 2008. The accuracy and stability of quartz watches. Horol. J.: 57–59.
10. Khorsheed S M and Yaseen N M, 2021. Effect of square shaped acousto-optic modulators on the Bragg diffraction. J. Phys.: Conf. Ser. **1897**: 012074.
11. Pitt C W, Skinner J D and Townsend P D, 1984. Acousto-optic diffraction of optical guided waves in crystal quartz. Electron. Lett. **20**: 4–5.
12. Chang I C, 1974. Tunable acoustooptic filter utilizing acoustic beam walkoff in crystal quartz. Appl. Phys. Lett. **25**: 323–324.
13. Collins R W and Ferlauto A S. Optical Physics of Materials. In: Irene E G & Tomkins H G (Eds), Handbook of Ellipsometry. Norwich, NY: William Andrew, 2005.
14. Arteaga O, Canillas A and Jellison G E Jr, 2009. Determination of the components of the gyration tensor of quartz by oblique incidence transmission two-modulator generalized ellipsometry. Appl. Opt. **48**: 5307–5317.
15. Shaskolskaya M P. Acoustic Crystals. Moscow: Nauka, 1982.
16. Narasimhamurty T S, 1969. Photoelastic constants of a quartz. J. Opt. Soc. Amer. **59**: 682–686.
17. Landolt-Borstein. Zahlenwerte und Funktionen aus Naturwissenschaften und Technik. Neue Serie: Bd. I. Elastiche, Piezooptishe Konstanten von Kristallen. Berlin: Springer, 1971.
18. Konstantinova A F, Grechushnikov B N, Bokut B V and Valyashko E G. Optical Properties of Crystals. Minsk: Navuka i Tekhnika, 1995.

19. Martynyuk-Lototska I Yu, Mys O G, Akimov S V, Krupych O M and Vlokh R O, 2010. Acoustogyration diffraction of optical waves: case of SiO_2 and TeO_2 crystals. Opto-Electron. Rev. **18**: 137–149.
20. Magdich L N and Molchanov V Ya. Acoustooptic Devices and Their Application. Gordon and Breach Science Publishers, 1978.

Mys O., Adamenko D. and Vlokh R. 2023. Increase in the acousto-optic figure of merit in SiO_2 crystals due to optical activity. Anisotropic acousto-optic interactions. Ukr.J.Phys.Opt. 24: 262 – 275. doi: 10.3116/16091833/24/3/262/2023

Анотація. *Проаналізовано анізотропну акустооптичну (АО) взаємодію трьох можливих акустичних власних хвиль із падаючою та дифрагованою оптичними власними хвилями, еліптично поляризованими завдяки явищу оптичної активності в кристалах кварцу. Одержано залежності ефективного пружнооптичного (ПО) коефіцієнта та коефіцієнта АО якості від кута дифракції. Продемонстровано, що належне врахування ненульової еліптичності оптичних власних хвиль приводить до відмінних від нуля значень деяких ефективних ПО коефіцієнтів та наявності відповідних АО взаємодій, які відносять до т. зв. типів VII і VIII. Виявлено також вплив неортогональності акустичних хвиль на ефективний ПО коефіцієнт та коефіцієнт АО якості при АО взаємодіях типів VII і VIII. Еліптичність оптичних власних хвиль проявляється в пікоподібних кутових максимумах ефективного ПО коефіцієнта та коефіцієнта АО якості для всіх типів розглянутих нами АО взаємодій. Ці максимуми з'являються навколо кутів дифракції 0 і 180 град, які відповідають колінеарній АО взаємодії між циркулярно поляризованими оптичними хвилями, що поширюються вздовж оптичної осі. Максимальні значення коефіцієнта АО якості в цьому разі дорівнюють відповідно* 1.16×10^{-15}, 0.36×10^{-15} *and* 0.48×10^{-15} c^3*/кг для типів АО взаємодій VII, VIII і IX. Насамкінець показано, що відхилення кута падіння від 90° при АО взаємодіях типів VII і VIII приводить до занулення ефективного ПО коефіцієнта та коефіцієнта АО якості.*

Ключові слова*: акустооптична дифракція, дифракційна ефективність, анізотропна дифракція, кристали кварцу, оптична активність, еліптичність власних оптичних хвиль.*